การประชุมวิชาการเครือข่ายวิศวกรรมเครื่องกลแห่งประเทศไทยครั้งที่ 21
17-19 ตุลาคม 2550 จังหวัดชลบุรี

Maximum Speed Determination of Composite Solid Disks

Sontipee Aimmanee[1*]

[1] Mechanical Engineering Department, Faculty of Engineering,
King Mongkut's University of Technology Thonburi,
Thung-kru, Bangkok, 10140, Thailand,
Tel: 0-662-470-9108, Fax: 0-662-470-9111, *E-mail: sontipee.aim@kmutt.ac.th

Abstract

In this paper, the determination for maximum speed or burst speed of laminated composite solid disks is presented. The disks, which are stacked in quasi-isotropic configuration herein, are taken into consideration. The virtual axisymmetry of the disks' geometry and physical properties provides circumferentially uniform behavior and facilitates an analysis of the disks' failure. The classical lamination theory (CLT) is employed to evaluate the smeared isotropic properties of the rotating composite disks. The overall radial and hoop stresses then can be determined by utilizing an elasticity solution of rotating isotropic circular plate. The stresses in the material coordinate along the fiber and transverse to fiber are computed via the law of tensorial transformation. By obeying the linear constitutive model, the corresponding strains can be obtained at particular rotational speed. The maximum angular velocity that specifies the disks' failure is noted when the strain components developed in the whole disk are reaching the ultimate strain values. The calculated burst speeds are also compared with experiments. Fairly good agreements are obtained in the case of S-glass epoxy and graphite epoxy composite disks. In addition, the present analysis results are compared with those computed from a simple mean hoop stress theory and their values are in the same order.

Keywords: Composite, Disk, Burst speed, Flywheel, Maximum strain criterion

1. Introduction

In engineering applications, rotating disks or flywheels are wildly used to maintain an even angular speed of a machine or operate as an energy accumulator. The performance of a flywheel can be indicated by energy density, which is defined as the ratio of kinetic energy stored to the mass of the disk at the burst or maximum speed [1]. As can be seen from the definition of energy density, it is desirable to develop a lightweight flywheel that can spin at very high angular velocity and still maintain structural integrity. Composite materials are then the dominant solution of such a requirement as a result of ability to tailor material properties upon desire.

Generally, composite flywheels can be categorized into two types based on geometry, i.e. rim flywheels and disk flywheels. A rim flywheel is an annular wheel, which concentrates the rotor mass as much as possible in the relatively thin rim in order to increase the mass moment of inertia around the rotating axis. It can easily be built with the filament-winding technique and has a good advantage of exploiting the high unidirectional strength of fiber to withstand the major stress in the circumferential direction. The radial stress for composite rim flywheels is usually low and therefore, can be sustained by the transverse strength of the composite. In contrast, a disk flywheel looks like the flat round plate centrally connected to driving shaft. It has more mass moment of inertia around the rotating axis than a composite rim flywheel when consuming the same swept area. It is designed to reach higher values of the energy density with higher peripheral velocities in comparison with a rim-type rotor. However, the state of stresses in the disk is more complicated due to the emergence of comparatively higher radial stress. Furthermore, if the disk is made from a laminated orthotropic layer, the interfacial stresses causing delamination may be important and partially control the failure of the disk. This, consequently, influences the more complex failure modes of the composite disk flywheel.

At the beginning of composite flywheel study, a number of different flywheels have been identified and published by some researchers [1-5], Moreover, a recent review by Arnold, et al. [6] indicated lots of research and publications on composite flywheels during a couple past decades. This points to a significant growing in using and developing composite flywheels in engineering applications. To additionally stream in this demand, this paper will present another mean of analysis of composite solid disks. The main objective is to develop a fairly simple but favorably realistic model to predict composite disk stress-strain behaviors during operation, particularly damage in the disk that is capable of being generated at a high rotating speed and the highest possible speed the disk can sustain right before bursting. Moreover, the model developed can be used to aid an investigation of disk failure mechanism and to complement as a design

criteria of a composite solid disk.

2. Theory

2.1 Stress and strain state of rotating composite disk

As mentioned above, the state of stresses that could happen in a laminated composite disk is quite complicated. A three-dimensional model is the most appropriate to govern the real physical behavior of the rotating disk. Nonetheless, for the sake of simplicity it is possible to postulate some assumptions that make the analysis more tractable and at the same time obtain useful information. For instance, if the laminated disk is thin when compared to its diameter, the classical lamination theory is applicable and then the problem is now classified as a plane stress problem. Additionally, delamination can be neglected for preliminary analysis purpose. Moreover, if the stacking sequence is made such that the quasi-isotropy is achieved, then in overall, the disk behaves very much like an isotropic material, which provides material axisymetry besides the geometrical symmetry around the rotating axis.

According to the assumptions stated earlier, the effective material properties for quasi-isotropic symmetric laminate in a composite disk can be expressed as [7]

$$\begin{aligned} E_{eff} &= \frac{A_{11}A_{22} - A_{12}^2}{A_{22}h} \\ G_{eff} &= \frac{A_{66}}{h} \\ \nu_{eff} &= \frac{A_{12}}{A_{22}} \end{aligned} \tag{1}$$

where E_{eff}, G_{eff} and ν_{eff} are effective Young's modulus, effective shear modulus, and effective Poisson' ratio of the laminate, respectively, h the total thickness of the laminate. A_{ij}, when i,j = 1,2,6, are in-plane stiffnesses of each lamina and related to reduced stiffnesses as follows

$$A_{ij} = \sum_{k=1}^{N} \bar{Q}_{ij} \left(z_k - z_{k-1} \right). \tag{2}$$

In the above, N is the total number of laminae in the laminate. $\bar{Q}_{ij}$ are the transformed reduced stiffnesses and are defined by

$$\begin{aligned} \bar{Q}_{11} &= Q_{11}m^4 + 2\left(Q_{12} + 2Q_{66}\right)n^2m^2 + Q_{22}n^4 \\ \bar{Q}_{12} &= \left(Q_{11} + Q_{22} - 4Q_{66}\right)n^2m^2 + Q_{12}\left(n^4 + m^4\right) \\ \bar{Q}_{22} &= Q_{11}n^4 + 2\left(Q_{12} + 2Q_{66}\right)n^2m^2 + Q_{22}m^4 \\ \bar{Q}_{66} &= \left(Q_{11} + Q_{22} - 2Q_{12} - 2Q_{66}\right)n^2m^2 + Q_{66}\left(n^4 + m^4\right) \end{aligned} \tag{3}$$

where $m = \cos\alpha$, $n = \sin\alpha$, in which α is the angle between the global coordinate system X-Y and fiber-direction (or 1-axis) of composite flywheel at a given layer depicted in Figure 1. The Q_{ij}, as expressed in Equation (3), are reduced stiffnesses and are functions of the engineering constants as shown in Equation (4). E_1 and E_2 denoted in Equation (4) are in-plane extensional modulus of the composite material along the fiber and transverse to the fiber directions, respectively. The property G_{12} is in-plane shear modulus. In addition, ν_{12} and ν_{21} are major and minor Poisson's ratios, respectively, which are related through the well-known reciprocity relation [7].

$$\begin{aligned} Q_{11} &= \frac{E_1}{1-\nu_{12}\nu_{21}} \\ Q_{12} &= \frac{\nu_{12}E_2}{1-\nu_{12}\nu_{21}} = \frac{\nu_{21}E_1}{1-\nu_{12}\nu_{21}} \\ Q_{22} &= \frac{E_2}{1-\nu_{12}\nu_{21}} \\ Q_{66} &= G_{12} \end{aligned} \tag{4}$$

In addition, one can utilize the elasticity solution of an isotropic rotating disk derived in [8, 9] for the quasi-isotropic case. The state of stresses at a material point reads

$$\begin{aligned} \sigma_r &= \frac{3+\nu_{eff}}{8}\rho\omega^2(b^2 - r^2) \\ \sigma_\theta &= \frac{3+\nu_{eff}}{8}\rho\omega^2 b^2 - \frac{1+3\nu_{eff}}{8}\rho\omega^2 r^2 \\ \tau_{r\theta} &= 0 \end{aligned} \tag{5}$$

In the above, σ_r is effective radial normal stress in the whole composite solid disk, σ_θ effective circumferential normal stress, $\tau_{r\theta}$ effective in-plane shear stress, ρ the mass density, ω the angular velocity of the disk, b the radius of the disk, and r radial distance from rotating axis.

Consequently, employing the effective material properties stated in Equation (1), the effective stress state defined in Equation (5) has the relationship with in-plane effective strains in the radial and circumferential directions as follows

$$\begin{Bmatrix} \varepsilon_r \\ \varepsilon_\theta \\ \gamma_{r\theta} \end{Bmatrix} = \left[E\right]^{-1} \begin{Bmatrix} \sigma_r \\ \sigma_\theta \\ \tau_{r\theta} \end{Bmatrix} \tag{6}$$

where

$$\left[E\right] = \begin{bmatrix} \dfrac{E_{eff}}{1-\nu_{eff}^2} & \dfrac{\nu_{eff}E_{eff}}{1-\nu_{eff}^2} & 0 \\ \dfrac{\nu_{eff}E_{eff}}{1-\nu_{eff}^2} & \dfrac{E_{eff}}{1-\nu_{eff}^2} & 0 \\ 0 & 0 & G_{eff} \end{bmatrix} \tag{7}$$

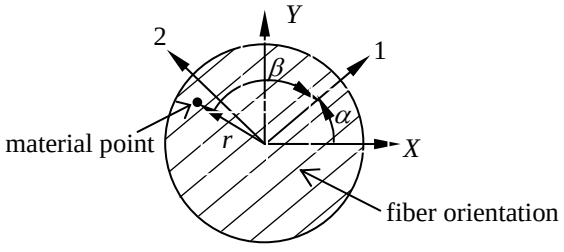

Figure 1. Global (X-Y) and material (1-2) coordinate systems of laminated composite disk

Note that the state of strains elaborated in Equation (6) does not exclusively signify its effective value but also provide the physical strains that actually occur in the laminated composite disk. This is because of the compatibility condition that constrains each lamina to displace equally when rotating. In addition, the strain state in the material coordinate system (or in-the-fiber and perpendicular-to-fiber directions) can be computed according to the rule of tensorial transformation as

$$\begin{Bmatrix} \varepsilon_1 \\ \varepsilon_2 \\ \gamma_{12} \end{Bmatrix} = \begin{bmatrix} p^2 & q^2 & 2pq \\ q^2 & p^2 & -2pq \\ -2pq & 2pq & p^2-q^2 \end{bmatrix} \begin{Bmatrix} \varepsilon_r \\ \varepsilon_\theta \\ \gamma_{r\theta} \end{Bmatrix} \tag{8}$$

Here, $p = \cos\beta$, $q = \sin\beta$, in which β is the angle measured from the radial line of a material point to the line of the fiber orientation.

Thus, the layerwise stress with respect to the material coordinate system can be calculated and expressed in Equation (9)

$$\begin{Bmatrix} \sigma_1 \\ \sigma_2 \\ \tau_{12} \end{Bmatrix} = \begin{bmatrix} Q_{11} & Q_{12} & 0 \\ Q_{12} & Q_{22} & 0 \\ 0 & 0 & Q_{66} \end{bmatrix} \begin{Bmatrix} \varepsilon_1 \\ \varepsilon_2 \\ \gamma_{12} \end{Bmatrix} \tag{9}$$

2.2 Failure analysis of laminated rotation disk

With the stresses in the material coordinate system calculated from Equation (9), the failure analysis can be performed in each lamina. The maximum strain criterion is employed herein in order to obtain the maximum speed of the rotating disk. Also, it can be observed that normal stresses in the rotating disk are always positive or in tension as indicated by Equation (5). Therefore, in accordance with the conditions set above, failure at a material point in the composite solid disk will occurs if at least one of the following equations of failure surface envelope satisfied

$$\begin{aligned} \varepsilon_1 &= \varepsilon_{XT} \\ \varepsilon_2 &= \varepsilon_{YT} \\ \gamma_{12} &= \gamma_{XY} \end{aligned} \tag{10}$$

where $\varepsilon_{XT}, \varepsilon_{YT}$ and γ_{XY} are ultimate tensile strains to failure in the 1 direction, in the 2 direction, and ultimate in-plane shear strain, respectively, of the material used in the laminated composite solid disk. However, Equation (10) may not be convenient to use in practice due to the limited available data of ultimate strains of composite materials. Thus, the another form of Equation (10) yet in stress format can be utilized as a substitute, which is expressed below

$$\begin{aligned} \sigma_1 + \frac{S_{12}}{S_{11}}\sigma_2 &= \sigma_{XT} \\ \sigma_2 + \frac{S_{12}}{S_{22}}\sigma_1 &= \sigma_{YT} \\ \tau_{12} &= \tau_{XY} \end{aligned} \tag{11}$$

In the above, S_{ij} when i,j = 1,2,6 are compliances of the composite material defined in Equation (12). σ_{XT}, σ_{YT} and τ_{XY} are ultimate tensile strengths in the 1 and 2 directions, and ultimate shear strength in the 1-2 plane, respectively.

$$S_{11} = \frac{1}{E_1}, S_{22} = \frac{1}{E_2}, S_{12} = -\frac{\nu_{21}}{E_2} \tag{12}$$

Mode of failure at a given material point can also be specified by considering which corresponding expression of Equation (11) is satisfied by the state of stresses at the point. Satisfaction of the first or second expression of Equation (11) indicates the failure in tension in-the-fiber direction or perpendicular-to-fiber direction, respectively. However, if the third expression satisfies, the failure occurs in shear mode in the 1-2 plane.

Consequently, by employing Equations (1)-(12), it is possible to introductorily determine the lowest spinning speed that causes damage at a material point (or a given pair of r and β values) in either failure mode discussed above. Also, the set of the aforementioned equations can basically determine the maximum rotating speed of the composite disk flywheel. This maximum rotating speed is defined as the speed that causes damage in at least one of the failure modes in every lamina throughout the whole disk. According to Equation (5), it is expected that the damage initially occurs at the center of the disk and subsequently spread to the outer radius of the disk when the rotating speed gets higher. The maximum speed or burst speed obtained from this approach provides fundamental information with respect to failure mechanism. However, it may be significantly overestimated due to negligence of damage accumulation within the flywheel before the damage spreading.

2.3 Ply discount method

As previously mentioned, the damage occurring during revolving propagates from center of the rotation to the circumference of the disk flywheel. The failure generated must affect the disk integrity owing to the material being broken. In reality, the failure is associated with a change in the stiffness of the laminate. Therefore, to get closer to the real physical phenomenon the ply discount method can be used in addition to the above calculation to account for the damage in material moduli as individual plies fail. In this method, the tensile or compressive modulus in the fiber direction of a lamina, which has undergone fiber breaking (or satisfaction of the first expression of Equation 10), is set to zero $(E_1 = 0)$ while the other moduli remain intact. On the other hand, when matrix cracking arises (or satisfaction of the second or third expression of Equation 10), both the transverse and shear moduli are set to zero $(E_2 = 0, G_{12} = 0)$ while the longitudinal modulus are the same. The action of discounting the relevant material properties in plies based on the occurring failure mode during performing the failure examination is called "progressive failure analysis".

3. Analysis procedures and results

The laminated disks used in the analysis are made of S-glass epoxy and graphite epoxy of which properties are tabulated as given in Table 1. [1,10]. The lamina thickness is 125×10^{-6} m. The laminate stacking sequence

of S-glass epoxy flywheel is $[0/ -45/ 45/ 90]_s$ with totally 200 laminae, and that of graphite epoxy disk is $[0/ 90/ 45/ -45]_s$ with totally 56 laminae. The radius, *b* of the S-glass epoxy and graphite epoxy flywheels are 11.27 cm and 16 cm, respectively. The quasi-isotropic stacking sequences and disks' radii are chosen in analysis because they are identical to the ones used in the experiment reported in [1] such that it is possible to compare the analysis results with the available experimental data.

Table 1: Lamina material properties for rotating disks

Properties	S-Glass Epoxy	Graphite Epoxy
E_1 (GPa)	48.95	144.8
E_2 (GPa)	10.0	9.65
G_{12} (GPa)	5.58	4.83
ν_{12}	0.3	0.3
ρ (kg/m^3)	2000	1630
σ_{XT} (MPa)	1500	1786.0
σ_{YT} (MPa)	54.1	48.3
τ_{XY} (MPa)	64.1	71.7

3.1 Without progressive failure analysis

From the material properties shown in Table 1, the failure analysis is performed without taking into account the ply discount method first. Thus, the decrease in the laminate modulus due to failure is ignored and the results will form an upper bound for the proposed failure mechanism.

The computational results show that the dominant failure mode of the laminated flywheels made from both types of material is matrix cracking because amongst all the solutions of obtained from Equation (11) that of the second equation yields the lowest failure angular speed at almost every position on the disks. The results indicate that matrix cracking initiates at the center the composite disk through the disk thickness at a certain speed. Then the damage propagates along the radius of the disk when the angular velocity keeps increasing as anticipated, since the magnitudes of radial and hoop stresses both are highest at the center point and start decaying when moving away from the rotating axis. The first angular velocity that creates the central point crack (defining herein as first-failure spinning speed or FFSS) is 4,153 rad/s and 4,832 rad/s for S-glass epoxy and graphite epoxy, respectively. In addition, it can be shown that at the same radial distance, *r* the minimum spinning speed that causes the matrix cracking is always at $\beta = 0^\circ$ in each lamina or equivalently the crack length is longest on the 1 axis (equal to 2*r* as shown in Figure 2) in the material coordinate system in each lamina and shortens when angle β is swept away from the 1 axis. This phenomenon happens because when angle β increases, the major part of the stresses is mainly distributed to fibers and then the chance of matrix cracking is reduced.

Also, at any running speed higher than FFSS the accumulated damage region within the flywheel forms elliptical shape on the 1-2 plane in each layer as portrayed in Figure 2. This elliptical shape has the 1-axis as major axis and 2-axis as minor axis. This elliptical damage zone has the same shape in all laminae, but its orientation may not coincide with that of other layers due to its probable difference of the material coordinate system from the others of the laminate. Additionally, the elliptical damage zone in each lamina can union altogether to approximately form a cylindrical damage volume (CVD) inside the composite disks as depicted in Figure 2. Furthermore, the maximum rotating speed in this case will be specified as the speed at which the cylindrical damage volume is equal to the whole disk volume. The results of speed-to-failure determination by excluding progressive failure analysis at any given radial distance, *r* are illustrated in Figures 3 and 4 for S-glass epoxy and graphite epoxy flywheels, respectively. Note that abscissa of the figures denoted by $\bar{r}$ indicates normalized radial distance *r/b*.

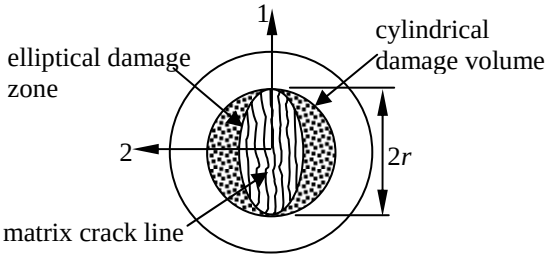

Figure 2. Elliptical damage zone in a lamina and cylindrical damage volume

3.2 With progressive failure analysis

By applying the ply discount method stated above, the progressive failure analysis can be conducted by discounting E_2 and G_{12} of the damaged laminae in CDV to zero due to the matrix cracking in this volume. Consequently, it appears that the flywheel with degraded moduli has two set of material properties. The outer part is original or undamaged material and then has the unchanged properties. However, the inner part is damaged so its properties are discounted. The effective properties of the damaged part are also assumed to be quasi-isotropic and can be calculated by using the same formulas stated in Equation (1). Nevertheless, the state of stresses in the original material is affected by the damaged material and thus, Equation (5) is no longer valid after discount method is employed.

Instead, the stress fields of the rotating disk with CDV can be obtained by solving a boundary value problem of a spinning compound cylinder. The elasticity solution of a disk subjected to a centrifugal force is: [9]

$$\sigma_r = \frac{E_{eff}}{1-\nu_{eff}^2}\left[\frac{-(3+\nu_{eff})(1-\nu_{eff}^2)\rho\omega^2 r^2}{8E_{eff}} + (1+\nu_{eff})c_1 - (1-\nu_{eff})\frac{c_2}{r^2}\right]$$
$$\sigma_\theta = \frac{E_{eff}}{1-\nu_{eff}^2}\left[\frac{-(1+3\nu)(1-\nu_{eff}^2)\rho\omega^2 r^2}{8E_{eff}} + (1+\nu_{eff})c_1 + (1-\nu_{eff})\frac{c_2}{r^2}\right] \quad (13)$$
$$u = -\frac{\rho\omega^2 r^2(1-\nu_{eff}^2)}{8E_{eff}} + c_1 r + \frac{c_2}{r}$$

E_{eff} and v_{eff} in the above has been defined in Equation (1). However, based on the progressive failure analysis there exist two sets of E_{eff} and v_{eff} in a laminated composite flywheel—the first set is the original value evaluated prior to discounting the material moduli and used in undamaged zone and the second one is the modified value after discounting the material moduli and used in CVD zone. c_1 and c_2 are unknowns that need to be determined and they also have two sets, the original and modified. Note that subscripts *org* and *mod* will be employed in the variables to follow to distinguish the difference between these two sets. In order to solve for four unknowns $c_{1,org}$, $c_{1,mod}$, $c_{2,org}$ and $c_{2,mod}$, boundary conditions expressed in Equation (14) below is utilized.

$$\begin{aligned} &\sigma_{r,mod} \text{ bounded at } r = 0 \\ &\sigma_{r,org} = 0 \text{ at } r = b \\ &\sigma_{r,org} = \sigma_{r,mod} \text{ at } r \text{ equal to CVD radius} \\ &u_{org} = u_{mod} \text{ at } r \text{ equal to CVD radius} \end{aligned} \tag{14}$$

With the solution of the four unknowns obtained it is possible to calculate stress distributions throughout the composite flywheel by using Equation (13). Consequently, Equations (1)-(4), (6)-(13) can be applied

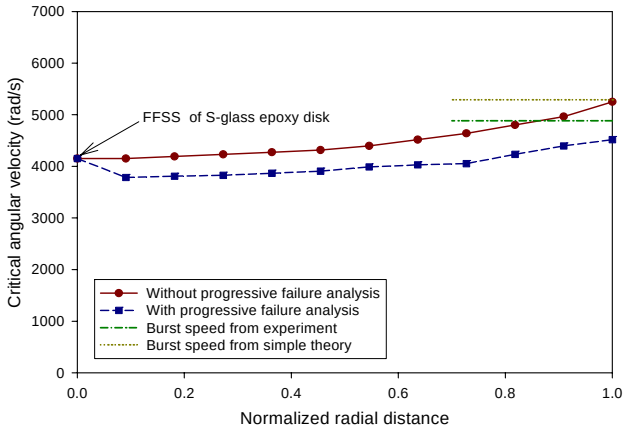

Figure 3. Critical angular velocity at any radial distance, $\bar{r}$ of S-glass epoxy disk

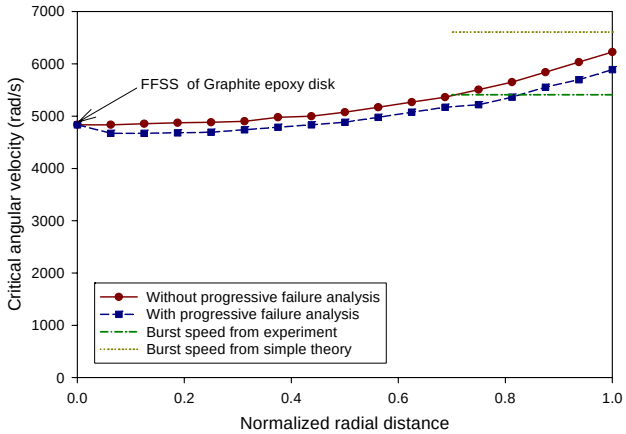

Figure 4. Critical angular velocity at any radial distance, $\bar{r}$ of the graphite epoxy disk

to determine critical rotating speed with progressive failure analysis at several sizes of CVD ranging from the center point to full size occupying the whole volume of the composite disk flywheel (or $0 \le r \le b$). The results are also depicted in Figures 3 and 4.

4. Discussions

As stated, Figures 3 and 4 illustrate the critical speed at any normalized radial distance of the S-glass epoxy and graphite epoxy composite disk flywheels. The plots illustrate that when the discounting technique is taken into account the critical rotating speed is lowered. This effect is associated with the fact that the interior degrading material with discounted properties continuously shifts the sustained load to the exterior undamaged material when the spinning rate gets faster and faster. This results in acceleration of failure generating in the undamaged zone.

Also, it should be noted that when the ply discount method is used, the crack region first starts at the center and rapidly sweeps over the 30-50% of the entire area of the disk (in the range of $0 \le \bar{r} \le 0.55 - 0.7$) if the rotating speed at FFSS or slightly over is maintained as shown in Figures 3 and 4. Furthermore, even though the maximum rotating speed is evaluated under the assumption of flywheel failure due to matrix cracking only, the analysis results reveal a fairly good agreement with experiments conducted in [10]. The probable reason is that the disk integrity is significantly affected by the matrix fracture and the binder may no longer hold the fibers together despite no fiber breaking involved in the failure.

However, the disagreement of the computed maximum rotating speed at $\bar{r} = 1$ and the bursting speed from experiments could be rendered by the imperfection in the fabricating process of the composite disks, the difference between the real materials' properties and the ones utilized in the analysis and the unexpected load from the imbalance vibration of the disks in the experiment.

As further comparison, a simple failure theory recently purposed by Kogo et al. [11] is adopted and modified to compute the maximum rotating speed of the composite disk flywheel and compare the results obtained with the analysis presented herein and the experimental data conducted by Nimmer [10]. They claimed that the hoop stresses is critical in the fracture of the composite disks and then the burst speed can easily be determined when mean hoop stress resultant, N_θ^{mean} is equal to the tension force per unit width that causes a specimen of the same composite material with identical stacking sequence to initially fail from the matrix cracking in a ply or so-called "first-ply failure". Accordingly, N_θ^{mean} can be defined as

$$N_\theta^{mean} = \frac{1}{b}\int_0^h\int_0^b \sigma_\theta \, dr dz \tag{15}$$

where σ_θ has been expressed in Equation (5). The tension force per unit width that causes first-ply failure due to matrix cracking in S-glass epoxy and graphite epoxy specimens with the same stacking sequences as the

flywheels will be determined by utilizing the maximum strain criteria discussed above. As a result, their values are equal to 5.93×10^6 N/m and 4.26×10^6 N/m for the S-glass epoxy and graphite epoxy specimens, respectively. By equating N_θ^{mean} to the obtained tension force per unit width, the maximum angular velocity can be evaluated and depicted in Figures (3) and (4). As shown, the simple failure theory overestimates the maximum rotating speed when compared to the presented analysis and the experiments. However, due to its straightforwardness, this simple failure theory can be used as a rough upper bound approximation of burst speed of laminated composite disk.

5. Conclusion

This paper has presented the maximum speed determination of laminated composite disk flywheels. The analysis was performed by using the maximum strain failure criterion with and without discounting material properties. The maximum angular velocities corresponding to the matrix cracking at any radial distance from the rotating axis can be computed. The maximum speeds of the laminated quasi-isotropic S-glass epoxy and graphite epoxy disks were determined and compared with the available experimental data. With the validation conducted herein, the developed model shows a good promise in real applications because it is realistic yet simple to apply.

However, it is interesting to calculate the maximum speed of the disks based on other failure criteria of anisotropic materials as well. This is to perceive their similarity and difference among the criteria for predicting failure of composite disk flywheels. Additionally, in practice, flywheels are also subjected to fatigue loads during the storing and discharging kinetic energy. Then, a fatigue investigation is needed in order to forecast the life of the flywheels in operation. Furthermore, delamination is another possible failure mode that might happen in laminated composite disks. Definitely, all of these effects are very important and should be taken into account when flywheel design is the issue.

Acknowledgments

The author would like to acknowledge Dr. Pattaramon Tantichattanont for proofreading this article and giving crucial comments to the author.

References

[1] Genta, G., 1985. Kinetic Energy Storage –Theory and practice of advanced flywheel system., Butterworths & Co Publishers Ltd.

[2] Keckler, C.R., Bechtel, R.T. and Groom, N.J., 1984. An Assessment of Integrated Flywheel System Technology, NASA CP 2346

[3] Post, R.F. and Post, S.F., 1973. Flywheels. Scientific American, USA

[4] Portnov, G.G., 1989. Composite Flywheels, Handbook of Composites: Structure and Design, Vol. 2. Elsevier, New York, USA

[5] Bitterly, J.G., 1998. Flywheel Technology, IEEE AES System Magazine, USA

[6] Arnold, S.M., Saleeb, A.F. and Al-Zoubi, N.R., 2002. Deformation and Life Analysis of Composite Flywheel Disk Systems. Composite: Part B, Vol. 33, pp. 433-459

[7] Hyer, M.W., 1980. Stress Analysis of Fiber-Reinforced Composite Materials., McGraw-Hill

[8] Timoshenko, S.P. and Goodier, J.N., 1970. Theory of Elasticity. 3rd ed., McGraw-Hill

[9] Ugural, A.C. and Fenster, S.K., 1994. Advanced Strength and applied Elasticity. 3rd ed., Prentice Hall

[10] Nimmer,R.P., 1980. Laminated, Composite Flywheel Failure Analysis. Flywheel Technology Symposium, Scottsdale, Arizona, October, pp. 445-457

[11] Kogo, Y., Hatta, H., Kawada, H., Shigemura, T., Ohnabe, H., Mizutani, and Tomioka, F., 1998. Spin Burst Test of Carbon-Carbon Composite Disk. Journal of Composite Materials, Vol. 32, No. 11, pp. 1016-1035